Polymer Chemistry

Accepted Manuscript

ROYAL SOCIETY OF CHEMISTRY

www.rsc.org/polymers

Journal Name

RSCPublishing

ARTICLE

Self-assembly and disassembly of redox-responsive ferrocene-containing amphiphilic block copolymer for controlled release

Lichao Liu, Leilei Rui, Yun Gao and Weian Zhang*

Cite this: DOI: 10.1039/x0xx00000x

Received 00th January 2014,
Accepted 00th January 2014

DOI: 10.1039/x0xx00000x

www.rsc.org/

Stimuli-responsive block copolymer micelles have recently emerged as promising drug delivery systems with controllable drug release. Herein, we report a well-defined redox-responsive ferrocene-containing amphiphilic block copolymer PEG-*b*-PMAEFc, which was synthesized by atom transfer radical polymerization (ATRP) of 2-(methacryloyloxy) ethyl ferrocene-carboxylate (MAEFc) using PEG-based macroATRP agent. This block copolymer can self-assemble into various interesting nanostructures in aqueous solution. The self-assembled morphology of amphiphilic block copolymers is influenced by the nature of common solvent, polymer composition and concentration, and the additives of β-cyclodextrin (β-CD) and redox agents (H_2O_2 and $KMnO_4$), which was investigated by transmission electron microscopy (TEM) and dynamic light scattering (DLS). Furthermore, the redox agent H_2O_2 can be used to trigger the release of encapsulated cargo (Rhodamine B) in polymeric nanocarriers. This redox behavior of the amphiphiles would open up an approach for redox-controlled drug delivery systems.

Introduction

Well-defined nanostructured materials self-assembled from amphiphilic block copolymers in aqueous solution have been widely investigated in the field of nanomedicine in the past few decades.[1-6] Stimuli-responsive polymeric materials, which can undergo physical or chemical changes in response to external stimuli, such as pH,[7-12] light,[13-17] temperature,[18-21] electricity,[22-24] CO_2,[25-29] and redox,[30-33] have received tremendous attention for biomedical applications in recent years. Among possible stimuli, redox-responsive polymers based on redox-active species, such as disulfide linkage[34-36] and supramolecular chemistry, [37-40] have attracted extensive attention in controlled drug encapsulation and delivery in physiological environments, where a continuous balance exists in the body between reactive oxygen species (ROS) production and antioxidants, especially for oxidative stress in cells.[41, 42] In addition, the more oxidative atmosphere intracellularly of inflammatory cells can be used to regulate the self-assembly behavior of redox-responsive amphiphilic block copolymers.[43] The design of redox-responsive block copolymer usually involves incorporation of redox-responsive centers in the polymer main chain, in the side groups or as cross-linking moieties for construction of redox responsive gels. Recently, Xu *et al.* has developed a series of well-defined selenium/tellurium-containing amphiphilic block copolymers for potential application as redox-responsive drug delivery vehicles and artificial enzymes.[44-47] To date, various interesting redox-responsive polymer systems are being extensively investigated and exploited for biomedical applications and materials chemistry.

Recent advances in polymer synthesis and bottom-up self-assembly approaches have significantly paved the way toward rationally designing block copolymers with tailored functionality and well-defined nanostructures. Metal-containing block copolymers are attracting extensive attention due to their novel physical properties and emerging applications ranging from biomedicine, biosensors, actuators, semiconductive materials, photovoltaic materials and catalysis.[48-50] Ferrocene-containing polymers, the first example for incorporation of metals into polymers with ferrocenyl moieties covalently bonded to polymer side-chain or main-chain, have been well-studied for decades by controlled living polymerization techniques. For example, Manners and Winnik recently presented the preparation and self-assembly behavior of main-chain ferrocene-containing functional nanomaterials based on polyferrocenyl-silanes (PFS) by living ring-opening polymerization with well-defined nanostructures *via* crystallization-driven self-assembly in solution.[51-55] In addition, Tang, Huang and their co-workers have constructed a series of well-defined ferrocene-containing block copolymers and amphiphilic homopolymers by controlled/living radical polymerization such as atom-transfer radical polymerization (ATRP) and reversible addition fragmentation transfer (RAFT) polymerization techniques, and obtained a variety of morphology-controlled assembled nanostructures.[56-62]

In the field of redox-responsive polymer systems, ferrocene is widely used as a hydrophobic building block to construct amphiphilic block copolymers for reversible self-assembly and controlled drug release. For example, Lu and coworkers synthesized O-benzylhydroxylamine-conjugated amphiphilic

block copolymer poly(ethylene oxide)-*b*-poly(2-formal-4-vinylphenyl ferrocenecarboxylate) (PEG-*b*-PFVFC) by RAFT polymerization which exhibited reversible redox-responsive self-assembly.[63-64] Crespy *et al.* prepared functional nanocapsules composed of a PVFc-*b*-PMMA block copolymer shell and a hydrophobic liquid core by living anionic polymerization, which can be selectively oxidized and used to release a hydrophobic payload by an oxidation reaction for redox-responsive release.[65] Nevertheless, in practical applications, the biocompatibility of PVFc-*b*-PMMA system is not so good due to its strong hydrophobicity and surfactant-assisted miniemulsion preparation technique. Manners and Winnik et al. reported the redox-triggered self-assembly of a series of amphiphilic diblock copolymers with hydrophobic polydimethylsiloxane (PDMS) or polystyrene (PS) block and hydrophilic organometallic polyferrocene polyelectrolyte block (PFS) in solution.[66-67] The amphiphilic diblock copolymers can reversibly self-assemble and disassemble into redox-active vesicles or spherical micelles. Moreover, as one type of redox-active guest, ferrocene and its derivatives have been widely used for the construction of redox- or electrochemical-responsive supramolecular systems *via* host-guest interactions with different host molecules, mainly including cyclodextrins, cucurbiturils, pillararenes and calixarenes.[68-71] Particularly, hydrophilic *β*-cyclodextrin (*β*-CD) can form thermally stable inclusion complexation with ferrocene group in aqueous solution, driven by hydrophobic interactions and the complementary character of size and shape between their structures.[72] Meanwhile, cyclodextrins-based host-guest interactions could be employed to control the bottom-up self-assembly behavior of ferrocene-containing block copolymers, and to construct redox-responsive supramolecular hydrogels. Harada *et al.* reported the formation of redox-responsive supramolecular polymeric hydrogels using inclusion complexes between β-CD and ferrocene group as supramolecular crosslinkers, which exhibited self-healing and self-repairing properties, and can be applied to artificial muscles. [31, 40] Very recently, Yuan *et al.* designed two end-decorated homopolymers which can orthogonally self-assemble into a supramolecular diblock copolymer in aqueous solution based on the terminal host-guest interactions between CDs and ferrocene molecules for electrochemical-responsive drug delivery. [73-76] To our best knowledge, the self-assembly behavior of ferrocene-containing amphiphilic block copolymers has not been systematically studied *via* tuning of the nature of common solvent, polymer composition and concentration, the additives of host molecules and redox agents. Especially, few reports have been described using biocompatible poly (ethylene glycol) as the hydrophilic building block, which can minimize unexpected accumulation in normal tissue as a strategy to improve the pharmacokinetics of drug delivery systems.[77-78]

Herein, we report a facile approach to fabricate redox-responsive ferrocene-containing amphiphilic block copolymer PEG-*b*-PMAEFc *via* ATRP using PEG-based macroATRP agent (**Scheme 1**). The self-assembly behavior of the block copolymer was investigated by transmission electron microscopy (TEM), and dynamic light scattering (DLS). The self-assembled nanostructures of PEG-*b*-PMAEFc block copolymers in aqueous solution were systematically investigated, which are dependent on the nature of common solvent, polymer composition and concentration, the additives of oxidants (H_2O_2 and $KMnO_4$) and host molecule β-cyclodextrin (β-CD). A variety of interesting hierarchical nanostructures were observed including vesicles, flowerlike vesicles, large compound micelles (LCMs), interconnect-vesicles and mesoporous-like vesicles. Furthermore, redox agents can be used to trigger the release of encapsulated cargo (RB) in this polymeric nanocarrier.

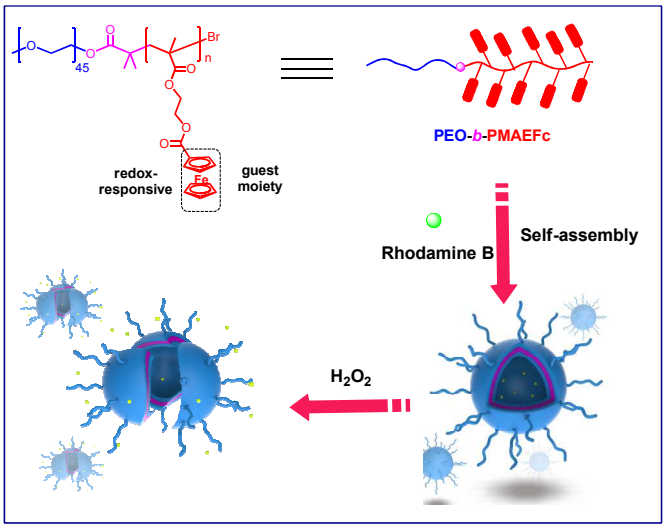

Scheme 1. The self-assembly of ferrocene-containing block copolymers PEG-*b*-PMAEFc, and the redox-responsive release of model molecule (Rhodamine B).

Experimental

Materials

2-Hydroxyethyl methacrylate (HEMA, 95%) was purified by passing through a basic alumina column and removing solvent afterward under reduced pressure. THF was refluxed with sodium chips under N_2 before use. Dimethyl formamide (DMF) and dimethylsulfoxide (DMSO) were dried over calcium hydride before use. Copper (I) bromide (Cu(I)Br, Sigma-Aldrich) was purified by stirring in acetic acid three times, then washed with ethanol, and dried under vacuum. *N, N'*-Dicyclohexylcarbodiimide (DCC), 4-(dimethyl amino) pyridine (DMAP), ferrocenecarboxylic acid, ascorbic acid, *N, N, N', N', N''*-pentamethyldiethylenetriamine (PMDETA), methoxy poly (ethylene glycol) (PEG, M_n = 2000), Rhodamine B (RB) and 2-bromoisobutyryl bromide were all purchased from Aladdin Reagents of China and used directly as received. β-Cyclodextrin (Shanghai Seebio Biotechnology, Inc., China) was recrystallized three times from deionized water. All other reagents were from commercial resources and used as received unless otherwise noted.

Characterization

^{1}H NMR and ^{13}C NMR spectra were recorded at 400 MHz, using BRUKER AV400 Spectrophotometer in $CDCl_3$ or DMSO-d_6 with tetramethylsilane (TMS) as an internal reference. The absorption spectra of all products were recorded on an AVATAR 360 ESP FT-IR spectrometer and the results were collected at 30 scans with a spectral resolution of 1 cm^{-1}. HR-MS was measured by a Waters LCT Premier XE spectrometer instrument. Elemental analysis was performed on a vario EL III Element Analyzer. Melting point was recorded at DIAMOND DSC. The sample (3-5 mg) was heated in nitrogen at a rate of 10 °C/min from 50 to 300 °C. The number

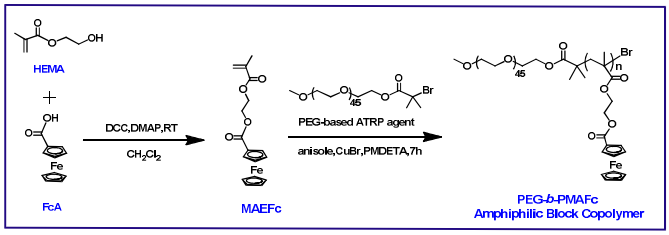

Scheme 2. The synthetic strategies of ferrocene-containing block copolymers PEG-*b*-PMAEFc.

average weight (M_n) and polydispersity index (PDI) was determined using a Waters 1515 gel permeation chromatograph (GPC) equipped with refractive index detector and ultrastyragel columns of 100-10 000 Å porosities. The GPC system was calibrated with polystyrene as the standards and tetrahydrofuran (THF) as the eluent at a flow rate of 1 mL min^{-1}. The UV-Vis spectra of the samples were measured over different irradiation time intervals by using a Thermo Scientific Evolution 220 spectrophotometer. Dynamic light scattering (DLS) measurements were carried out at BECKMAN COULTER Delasa Nano C particle analyzer, and all the measurements were carried out at room temperature. Transmission electron microscopy (TEM) analysis was performed on a JEOL JEM1400 electron microscopes operated at 100 kV. High resolution transmission electron microscopy (HR-TEM) analysis was performed on a JEOL JEM2100 electron microscopes operated at 200 kV. Samples for TEM and HR-TEM were prepared by dropping the micelle solution onto a carbon-coated copper grid and then dried at room temperature. The scanning electron microscopy (SEM) analysis was performed on a field emission microscope (S-4800, HITACHI) with the accelerating voltage of 15.0 kV. The samples were sputtered by gold before the observation.

Synthesis of monomer 2-(methacryloyloxy) ethyl ferrocene carboxylate (MAEFc)

Ferrocenecarboxylic acid (2.02 g, 8.78 mmol), 2-hydroxyethyl methacrylate (HEMA) (0.85 g, 10.72 mmol) and 4-(dimethylamino) pyridine (0.13 g, 1.06 mmol) were dissolved in 100 mL of anhydrous dichloromethane (DCM). The mixture was cooled to 0 °C in an ice-water bath under N_2 flow and stirred for 30 min. Then, *N, N'*-dicyclohexylcarbodiimide (DCC, 2.15 g, 10.43 mmol) in anhydrous DCM (20 mL) was added dropwise to the above solution at 0 °C for 1 h. After the addition was completed, the mixture was stirred at 0 °C for another 1 h and then 24 h at room temperature. After removing the insoluble salts by suction filtration, the filtrate was concentrated and further purified by silica gel column chromatography using petroleum ether/ethyl acetate (12/1, v/v) as the eluent. After removing the solvents by a rotary evaporator, the final product MAEFc was obtained as a yellow solid (1.91 g, yield: 95%). ^{1}H NMR (400 MHz, $CDCl_3$, δ): 1.98 (s, -C*H*$_3$), 4.19 (s, -C*H*- in ferrocene group), 4.41 (m, -C*H*- in ferrocene group), 4.46 (s, -OCH_2CH_2O-), 4.81 (s, -C*H*- in ferrocene group), 5.62 (s, -C*H*), 6.19 (s, -C*H*). HR-MS (EI, *m/z*): $[M + H]^+$ calcd for $C_{17}H_{19}O_4Fe$, 342.0554; found, 342.0550. Anal. Calcd: C, 59.67; H, 5.30; Found: C, 59.46; H, 5.09.

Synthesis of amphiphilic block copolymer PEG-*b*-PMAEFc

The typical procedure for the synthesis of amphiphilic diblock copolymers PEG-*b*-PMAEFc *via* ATRP using PEG-based macroATRP initiator is described below: A 25 mL reaction flask equipped with a magnetic stirring bar and a rubber seal was charged with PEG-Br (0.1 g, 0.05 mmol), MAEFc (0.51 g, 1.5 mmol), PMDETA (43.5 mg, 0.25 mmol), and anisole (3 mL). After purging with nitrogen for 30 min to eliminate the oxygen, CuBr (43.2 mg, 0.30 mmol) was then introduced under N_2 flow to start the polymerization at room temperature under a nitrogen atmosphere. The polymerization was performed at 90 °C for 7 h in an oil bath. At the end of the reaction, the polymerization was terminated by exposing to air and diluting with THF. The reaction mixture was passed through a neutral alumina column to remove copper catalysts. After removing solvents by a rotary evaporator, the residues were dissolved in THF and precipitated twice into an excess of diethyl ether to remove residual monomer. The final product was dried in a vacuum oven overnight at 50 °C, yielding an orange solid (0.81 g, yield: 13.0%, $M_{n,\ GPC}$ = 4 248, M_w/M_n = 1.11). ^{1}H NMR (400 MHz, $CDCl_3$, δ): 0.90-1.44 (m, -C*H*$_3$ in PMAEFc), 1.81-2.10 (m, -CH_2-), 2.24 (s, -C*H*$_3$), 3.40 (s, C*H*$_3$O-), 3,67 (s, - OCH_2CH_2O-), 4.22 (s, -C*H*- in ferrocene group), 4.32-4.50 (m, -C*H*- in ferrocene group and -OCH_2CH_2O- in PMAEFc), 4.22 (s, -C*H*- in ferrocene group).

Fabrication of PEG-*b*-PMAEFc micelles in water

The micellar solution was prepared by the following process: 5 mL of deionized water was slowly dropped into 1 mL solution of 2.5 mg mL^{-1} PEG-*b*-PMAEFc in THF under vigorous stirring. THF was removed by dialysis (MWCO=12 000 Da) against deionized water, and fresh deionized water was replaced every 6 h. After 48 h, the volume of the solution was increased to 8 mL to obtain the micellar solution with a concentration of 0.3 mg mL^{-1} for further experiments.

Redox reactions of PEG_{45}-*b*-$PMAEFc_{38}$ vesicles

The aqueous vesicles dispersions (4 mL, 0.3 mg mL^{-1}) were divided in two equal parts, and treated with slight molar excess of H_2O_2 and $KMnO_4$ compared to the total ferrocene units in diblock copolymer PEG_{45}-*b*-$PMAEFc_{38}$, respectively. Afterward, the dispersions were stirred for 24 h and dialyzed (MWCO = 12 000 Da) against deionized water for 48 h. Subsequently, the vesicles dispersions oxidized by H_2O_2 and $KMnO_4$ were separately reduced by addition of an excess of ascorbic acid and stirred for 48 h at room temperature.

Encapsulation and oxidation-responsive release of RB

RB-loading micelles were prepared according to the literature: [65] 0.1 mg RB powder and 2.5 mg PEG_{45}-*b*-$PMAEFc_{38}$ block copolymer were together dissolved in 1 mL DMSO. Upon stirring, 5 mL of deionized water was added dropwise in 2 h. DMSO was then removed by dialysis (MWCO = 12 000 Da) against deionized water for 48 h and fresh water was replaced every 6 h to ensure complete remove of excess RB molecules that failed to be entrapped by polymer vesicles. The final concentration of polymer is 0.3 mg mL^{-1}. For the release experiments, 2 mL of RB-loaded PEG_{45}-*b*-$PMAEFc_{38}$ vesicles with a concentration of 0.3 mg mL^{-1} was mixed with 0.1 mL of 30% H_2O_2 so that the final concentration of H_2O_2 is 1.4 %. The vesicular solution was then dialyzed against deionized water in a beaker with same concentration of H_2O_2 to conduct the release experiments. A 2 mL portion of deionized water solution was withdrawn from the beaker at certain time intervals. The solution was then placed into a cuvette to measure fluorescence spectrum.

The release rate of RB was calculated based on the fluorescence intensity.

Results and discussion

Among a variety of organometallic polymers, metallocene-containing polymers have been readily available as interesting building blocks in advanced materials science due to their unique properties and functions in the fields of catalysis, batteries, sensors, magnetic materials, lithography, and biomedical systems such as controlled release.[65] Ferrocene-containing polymers, with ferrocenyl substituents in polymer side chains, were the first example for introduction of metals into polymers.[48] Since then, macromolecules including dendrimers, peptides, and polysaccharides, functionalized with metallocene moieties, have attracted significant attention, even for some polymers with well-defined architectures such as block copolymers over the past decades. [49-50, 79] The development of "living"/controlled radical polymerization, such as reversible addition-fragmentation chain transfer (RAFT) polymerization [80] and atom transfer radical polymerization (ATRP), [81] provides opportunities to prepare well-defined metal-containing polymers with complex architectures. Additionally, self-assembly is ubiquitous in nature and daily life, which is not limited to metal-containing block copolymer and helps to create self-organized, functional materials with interesting properties and extraordinary self-assembled hierarchical nanostructures. The synthesis procedures and factors influencing the self-assembly behavior of ferrocene-containing block copolymer including the nature of the common solvent, polymer composition and concentration, the addition of host molecule β-cyclodextrin (β-CD) and oxidants (H_2O_2 or $KMnO_4$), and the redox-responsive release process of the system are described in detail below.

Synthesis of ferrocene-containing block copolymers PEG-*b*-PMAEFc

Ferrocene was chosen as a redox-responsive moiety due to its simple oxidative-active behavior, and thermally stable inclusion complexation by β-CD. The facile pathway to synthesize ferrocene-containing monomer for living polymerization techniques has been reported widely.[56-62, 82-83] MAEFc monomer containing ferrocenyl motifs was readily synthesized *via N, N'*-dicyclohexylcarbodiimide (DCC) coupling reaction between ferrocenecarboxylic acid and HEMA (**Scheme 2**). The MAEFc was characterized by ^{1}H NMR, ^{13}C NMR, elemental analysis, HR-MS and FT-IR (**Fig. S1-S5**), respectively. As shown in the ^{1}H NMR, the peaks at 4.2, 4.4 and 4.8 ppm were corresponding to the signals of the protons in cyclopentadienyl (Cp) rings of the ferrocene unit, while the signals at 5.6 and 6.2 ppm were assigned to the double bond of the methacrylate group. The signals at 2.0 and 4.5 ppm were ascribed to the methyl protons and methylene protons respectively. ^{13}C NMR spectrum of MAEFc is shown in **Fig. S2**, and the peak at 18.2 ppm was assigned to one carbon of the methyl group. The peaks from 69.8 to 71.5 ppm were corresponding to the signals of 10 carbons in cyclopentadienyl (Cp) rings of the ferrocene unit. The signals at 167.2 and 171.6 ppm were attributed to two carbons of the carbonyl group, while the signals at 126.1 and 136.0 ppm were assigned to the two carbons of the double bond. The signals of two carbons of OCH_2CH_2O were found at 62.0 and 62.7 ppm, respectively. Furthermore, HR-MS afforded the formula of $C_{17}H_{19}O_4Fe$, and the found mass was 342.0550, which was lower than the calculated mass of 342.0554 because of Fe isotope effect (**Fig. S3**). The melting point of MAEFc is 77.2 °C, which was measured by differential scanning calorimeter (DSC) as shown in **Fig. S4**. In addition, all peaks of the FT-IR as shown in **Fig. S5a** were well matched with the structure of MAEFc. Thus, FT-IR spectrum further confirmed MAEFc was successfully prepared.

Here, the ferrocene-containing monomer MAEFc was further used to construct PEG-*b*-PMAEFc amphiphilic block copolymers with ferrocene moieties in the hydrophobic block via ATRP using PEG-based macroATRP initiator. ATRP is one of the most powerful and versatile techniques for the design and synthesis of new polymeric materials with well-defined structures since it is effective for a wide range of functional monomers and does not require stringent reaction conditions. [81] Previous results have shown that brominated polyethylene glycol (PEG-Br) macroinitiator was facilely prepared *via* esterification reaction of bromoisobutyryl bromide with PEG. Zhu *et al.*[84] reported the preparation of well-defined azobenzene-containing amphiphilic diblock copolymer using a PEG-based macroATRP agent. Tang *et al* [59] prepared a mono-functional ATRP macroinitiator based on PEG for chain extension with ferrocene-containing monomer MAEFc and styrene to fabricate triblock copolymer PEG-*b*-PMAEFc-*b*-PS, which was used for template synthesis of ordered iron oxide nanoparticles. In present work, ATRP polymerization of MAEFc monomer was performed using CuBr/PMDETA as the catalyst system and PEG-Br as an initiator to produce well-defined amphiphilic PEG-*b*-PMAEFc block copolymer, and the results are summarized in **Table 1**.

Table 1. Molecular weights, molecular weight distributions of amphiphilic block copolymers PEG-*b*-PMAEFc

block copolymers	DP[a]	$M_{n,NMR}$ (KDa)[a]	$M_{n,GPC}$ (KDa)[b]	M_w/M_n[b]	Wt% PMAEFc[b]
PEG_{45}-*b*-$PMAEFc_{12}$	12	6.0	4.2	1.11	52.4
PEG_{45}-*b*-$PMAEFc_{38}$	38	15.2	9.6	1.27	79.2
PEG_{45}-*b*-$PMAEFc_{49}$	49	18.7	13.5	1.33	85.2

[a]Number averaged molecular weights of diblock copolymers and average degrees of polymerization (DPs) for the PMAEFc block were determined by ^{1}H NMR. $M_{n,NMR} = [M]_0/[I]_0 \times M_{MAEFc} \times x + M_{init.}$, where M_{MAEFc} and $M_{init.}$ are the molecular weights of MAEFc and macroATRP initiator, respectively, x is the conversion, as measured by ^{1}H NMR. [b]Molecular weights, molecular weight distributions, M_w/M_n, and weight fraction of PMAEFc block were evaluated by GPC with polystyrene standards.

^{1}H NMR spectrum was utilized to determine the performance of the polymerization of ferrocene-containing monomer MAEFc. The resonance signals of double bonds in the ^{1}H NMR spectrum disappeared while the resonance signals from Cp rings of ferrocene moiety still appeared (**Fig. 1a**). The number averaged molecular weights of diblock copolymers and average degrees of polymerization (DPs) for the PMAEFc block were determined from ^{1}H NMR analysis of the final products by comparing the resonance signals of methyl groups at the end of PEG (3.4 ppm) and the resonance signals from Cp rings (4.2-4.8 ppm) as summarized in **Table 1**. Block copolymer PEG-*b*-PMAEFc was also well characterized by FT-IR spectrum (**Fig. S5b**). The characteristic signals of PAEFc block appeared at

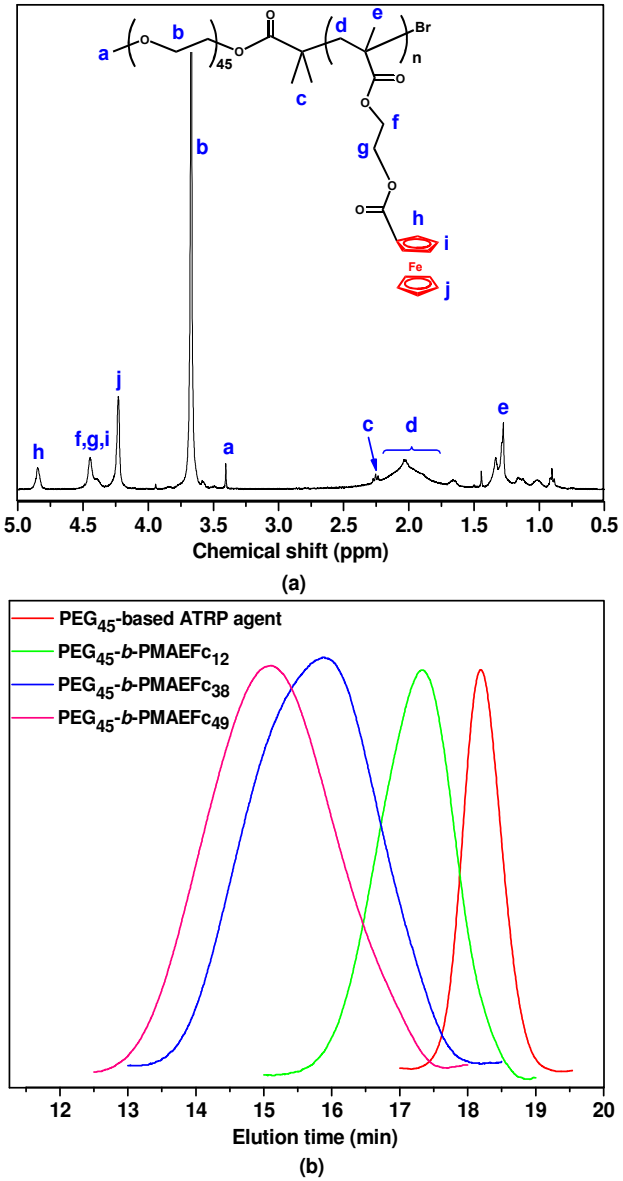

Fig. 1. ^{1}H NMR spectrum of PEG_{45}-*b*-$PMAEFc_{38}$ (a), and GPC traces of PEG-based macroATRP initiator and amphiphilic block copolymer PEG-*b*-PMAEFc (b).

2906, 1708, 813 cm^{-1}. Moreover, the molecular weight of the diblock copolymer was evaluated by GPC. Three amphiphilic diblock copolymers with varying DPs of PMAEFc block, PEG_{45}-*b*-$PMAEFc_{12}$, PEG_{45}-*b*-$PMAEFc_{38}$, and PEG_{45}-*b*-$PMAEFc_{49}$, were synthesized with narrow molecular weight distributions ($M_w/M_n \leqslant 1.33$) (**Fig. 1b**), which is consistent with the living polymerization characteristic of ATRP and demonstrated the well-defined ferrocene-containing block copolymers were successfully prepared.

Self-assembly behavior of ferrocene-containing amphiphilic block copolymers PEG-*b*-PMAEFc

With both a hydrophilic segment and a hydrophobic segment, block copolymers often show an amphiphilic character that they can self-assemble into a variety of interesting nanostructures with diverse morphologies including spheres, cylinders, vesicles, lamellae, large compound micelles (LCMs), and hierarchical assemblies in solution.[1, 85] In current work, PEG-*b*-PMAEFc diblock copolymers with inherent amphiphilic nature is expected to self-assemble interesting nanostructures in aqueous solution. The self-assembly process was triggered by adding water dropwise into a solution of PEG-*b*-PMAEFc in organic solvent to reduce the solubility of PMAEFc block, followed by dialysis against water to remove the organic solvents. The obvious bluish tint of the dispersions evidenced the formation of micelles. The critical micelle concentration (CMC) was determined by the pyrene fluorescence probe (**Fig. S6**). Interestingly, the morphologies of micelles fabricated from PEG-*b*-PMAEFc were dependent on the nature of common solvent, polymer composition and concentration, and the additives of oxidants and host molecule β-cyclodextrin (β-CD). The self-assembled nanostructures determined by above factors were further investigated in detail by transmission electron microscopy (TEM), dynamic laser scattering (DLS) measurements and UV spectroscopy in subsequent sections, respectively.

The nature of common solvent plays a critical role in the formation of self-assembled nanostructures, which can directly influence the stretching degree of hydrophilic and hydrophobic domains of the nanostructures. Therefore, we herein chose two different common solvents (DMSO and THF) to investigate the self-assembly of ferrocene-containing diblock copolymers in aqueous media with different polymer composition and concentration. To explore the effect of polymer composition (ratio of hydrophobic block to hydrophiphilic block) on the self-assembled structures, we prepared block copolymers with a constant PEG block and PMAEFc blocks of various chain lengths for our investigation. Using pure DMSO as the cosolvent, different types of typical nanostructures were achieved from PEG_{45}-*b*-$PMAEFc_n$ diblock copolymers *via* slow addition of water into the solution to trigger the self-assembly process. The final concentration of polymer solutions was 0.3 mg mL^{-1} by dialysis with water to remove the cosolvent. TEM and DLS were used to characterize the self-assembled morphologies of the three diblock copolymers. Interesting flower-like micelles of PEG_{45}-*b*-$PMAEFc_{12}$ were obtained as revealed by TEM images (**Fig. 2a**) with a diameter of 190 nm. Upon further increasing the hydrophobic chain length, uniform vesicles were obtained under similar conditions, exhibiting an average diameter of 250 nm (**Fig. 2b**). The brighter membrane should be the corona which is presumably formed by PEG block, while the thin and darker membrane should be the wall with the thickness of 11-12 nm which is served by hydrophobic PMAEFc block as shown in **Fig. S7**. The PMAEFc chain in PEG_{45}-*b*-$PMAEFc_{38}$ was calculated to be 10 nm if it adopts a rigid conformation. Therefore, the diblock copolymers could be packed in an interdigitated arrangement to form a bilayer vesicular structure. As reported by Zhu *et al*, the diblock copolymer PEG_{45}-*b*-$P(DMA\text{-}Azo)_{47}$ was thought to pack in an interdigitated arrangement to form a bilayer structure due to the H-type aggregate of DMA-Azo in the vesicles.[84] In current case, UV absorption spectrum was used to further investigate the self-assembly of PEG_{45}-*b*-$PMAEFc_{38}$. As shown in **Fig. 3**, the broad featureless spectrum of the vesicles in water is probably a result of the aggregation of ferrocene moieties which leads to a solid state-type spectrum i.e. the weak peak at 450 nm is broad so much that it is no longer detectable. The band at 275 nm in the spectrum is intrinsically much more intense in DMSO than water, which is associated with a π-electron transition of ferrocene. But it can still be detected in water, although it is broader and

weaker. Large compound micelles (LCMs) fabricated from PEG_{45}-*b*-$PMAEFc_{49}$ with longer PMAEFc block were also observed in **Fig. 2c**, with a diameter of 310 nm. Eisenberg *et al.*[86-87] found that large compound micelles were obtained during the self-assembly of PS_{200}-*b*-PAA_4 diblock copolymer with a diameter of more than 1 μm. The LCMs had a structure consisting of reverse micelles with short PAA as core and PS as corona, and PAA chains as the outer surface.

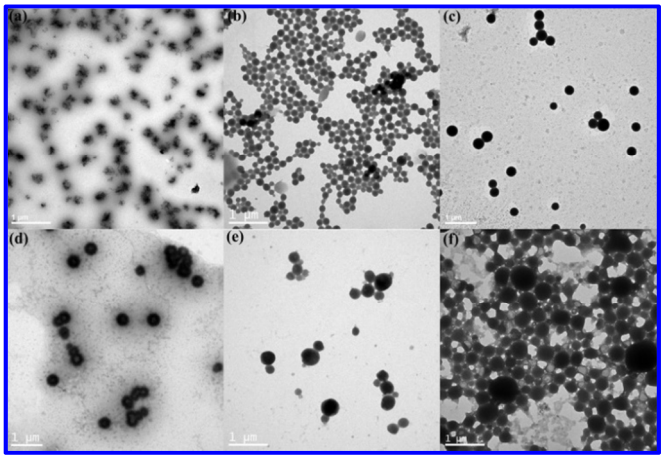

Fig. 2. TEM images obtained from PEG-*b*-PMAEFc block copolymers by varying polymer compositions (PEG_{45}-*b*-$PMAEFc_{12}$, PEG_{45}-*b*-$PMAEFc_{38}$ and PEG_{45}-*b*-$PMAEFc_{49}$) with DMSO (a-c) and THF (d-e) as the common solvent, respectively.

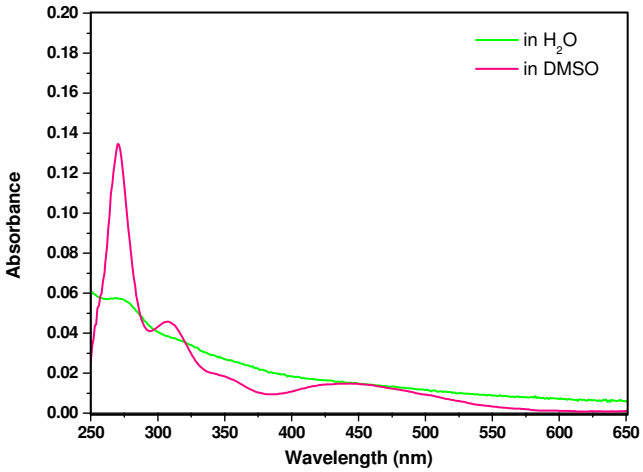

Fig. 3. UV/Vis spectra of PEG_{45}-*b*-$PMAEFc_{12}$ in DMSO and in H_2O (C = 0.05 mg mL^{-1}).

Similarly, THF was also chosen as the cosolvent to study the effect of polymer composition of PEG_{45}-*b*-PMAEFc diblock copolymers on their self-assembled morphologies in aqueous solution. Typical bilayer vesicles or polymersomes of PEG_{45}-*b*-$PMAEFc_{12}$ was obtained and revealed by TEM images (**Fig. 2d**) with a diameter of 250 nm. Upon further increasing the hydrophobic chain length, non-uniform spherical vesicles were obtained under similar conditions, exhibiting an average diameter of 300 nm (**Fig. 2e**). A similar phenomenon was also observed during the investigation of self-assembly of PEG_{45}-*b*-$PCPTM_{52}$ polyprodrug amphiphiles, in which flowerlike vesicles with a diameter of 790 nm were obtained. [88] The ferrocene-containing amphiphiles with longer PMAEFc block, PEG_{45}-*b*-$PMAEFc_{49}$, can also self-assemble into large compound micelles (LCMs) with a diameter of 370 nm as observed in **Fig. 2f**. The DLS results in **Fig. 4** showed that the average sizes of PEG_{45}-*b*-$PMAEFc_{12}$, PEG_{45}-*b*-$PMAEFc_{38}$, and PEG_{45}-*b*-$PMAEFc_{49}$ aggregates were 300 nm, 350 nm and 390 nm, respectively, which agreed well with TEM results. We can find that the diameter of the self-assembled nanostructures clearly changed by varying the chain length of hydrophobic blocks. As the PMAEFc chain became longer, the diameter the nanostructures increased. Therefore, the average size and morphology of self-assembled aggregates are sensitive to copolymer composition, namely the block length ratio between hydrophobic block and hydrophilic block, which is similar to the previous result reported by Eisenberg *et al.*[83] For spherical aggregates with increasing PMAEFc block length, the morphology changed from flower-like micelles to uniform vesicles to spherical LCMs with DMSO as the cosolvent, and from typical bilayer vesicles to non-uniform vesicles and to LCMs with cosolvent THF. The polymer composition-dependent morphologies reflect combined effects of hydrophobic ferrocene-containing block characteristics and kinetic control of self-assembling process. Considering the rigidness and crystalline of ferrocene moieties and hydrophobic nature of PMAEFc block, ferrocene-containing PMAEFc segments of block copolymer is highly ordered and closely packed within the internal corona of vesicles to form flower-like micelles with cosolvent DMSO, and bilayer vesicles with cosolvent THF. [54, 89] As the length of PMAEFc segments increase, an increase of the aggregation number is energetically favourable due to the decrease of interfacial area and energy between the cosolvent and PMAEFc segments. And the size of the vesicles increased as the increase of aggregation number. For the vesicles, the increase of PMAEFc chain stretching and the repulsion among the internal corona chains are thermodynamically unfavorable, which allows partial PMAEFc segments to be incorporated into the core of vesicles without significant changes in their morphology. Upon further increasing the hydrophobic chain length, this process continued to perform, and more PMAEFc segments were incorporated into the vesicle core, which resulted in the morphology transition from vesicles to LCMs and the increase of diameter of the spherical micelles. These results also verify that the self-assembly process is governed by the free energy of block copolymer aggregates. [85]

The effect of polymer concentrations in these two different cosolvents on the self-assembly morphologies was also respectively investigated. The self-assembled nanostructure was studied by DLS and TEM images with three kinds of copolymer concentrations. Vesicles with an average diameter of 110 nm were facilely obtained *via* addition of water into PEG_{45}-*b*-$PMAEFc_{38}$ solution in DMSO with a concentration of 0.1 mg mL^{-1} (**Fig. 5a**). When the concentration of PEG_{45}-*b*-$PMAEFc_{38}$ was increased to 0.3 mg mL^{-1}, vesicles were observed with an average diameter of 250 nm (**Fig. 5b**). As the concentration was further increased to 0.7 mg mL^{-1}, large compound micelles (LCMs) were obtained with larger size of 1 μm as shown in **Fig. 5c**. Employing similar fabrication procedures with THF as the cosolvent, large compound micelles (LCMs) with an average diameter of 250 nm determined by DLS were facilely obtained with a concentration of 0.1 mg mL^{-1} (**Fig. 5d**). Huang *et al*. found that amphiphilic homopolymers bearing ferrocene and carboxyl functionalities could form large compound micelles in water with relatively low initial copolymer concentration. [62] When the concentration of PEG_{45}-*b*-$PMAEFc_{38}$ was increased to 0.3 mg mL^{-1}, non-uniform vesicles were observed with an average

diameter of 350 nm determined by DLS as discussed above (**Fig. 4**). As the concentration was further increased to 0.7 mg mL^{-1}, compacted interconnected microstructures were obtained using THF cosolvent, where the vesicles have undergone a structural evolution including intense adhesion and fusion with the neighbouring ones, generating the interconnected microstructures as shown in **Fig. 5f**. These observations indicated that polymer concentrations have a significant influence on the self-assembled nanostructures. The morphologies changed from vesicles to LCMs with DMSO as the cosolvent, while from LCMs to non-uniform vesicles to interconnected microstructures with cosolvent THF. And the diameter of these nanostructures increased with increasing the copolymer concentration. We found that the increase of copolymer concentration can have a morphologic effect on the aggregates similar to that of increasing hydrophobic chain length, as previously reported by Eisenberg *et al* in the self-assembly of PS-b-PAA in aqueous solution. [85] The aggregation number increases with increasing copolymer concentration, which leads to an increase in the degree of ferrocene-containing hydrophobic blocks stretching and the core dimension to reduce the energy penalty.

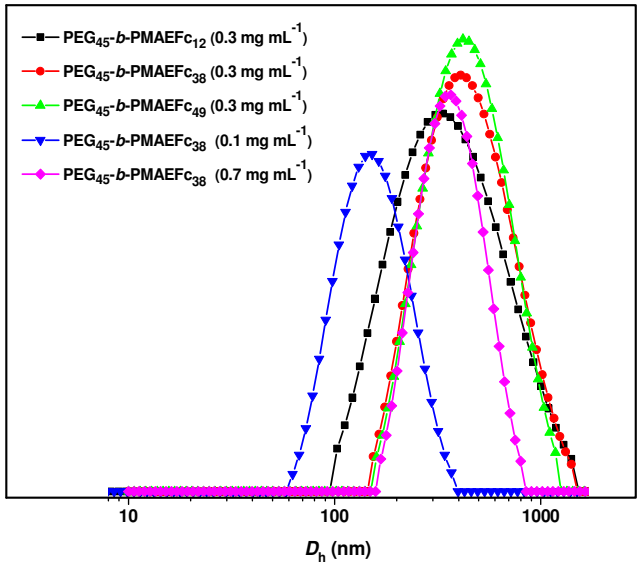

Fig. 4. DLS results of PEG-*b*-PMAEFc block copolymer by varying polymer compositions (PEG_{45}-*b*-$PMAEFc_{12}$, PEG_{45}-*b*-$PMAEFc_{38}$ and PEG_{45}-*b*-$PMAEFc_{49}$) and concentrations (0.1 mg mL^{-1}, 0.3 mg mL^{-1}, 0.7 mg mL^{-1}) with THF as the cosolvent.

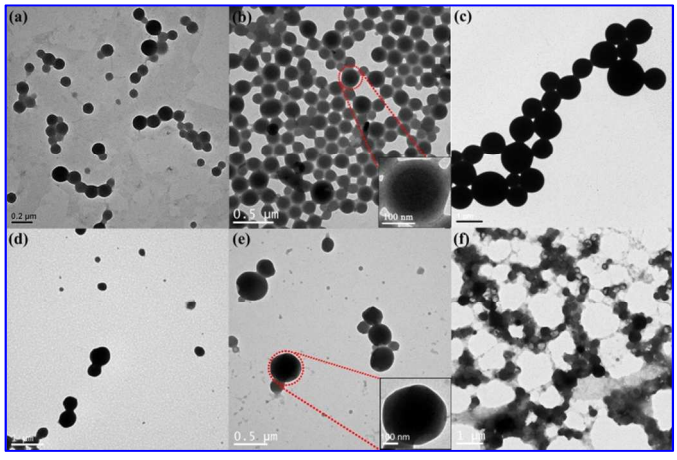

Fig. 5. TEM images obtained from PEG_{45}-*b*-$PMAEFc_{38}$ block copolymers by varying polymer concentrations (0.1 mg mL^{-1}, 0.3 mg mL^{-1}, 0.7 mg mL^{-1}) with DMSO (a-c) and THF (d-e) as the common solvent, respectively.

After systematic investigation of self-assembled morphologies by varying copolymer composition and concentration in different cosolvents (THF and DMSO), respectively, we found that the self-assembled nanostructures are greatly dependent on the nature of common solvent we used. The shape of the vesicles fabricated with DMSO as cosolvent was more uniform than that using THF as common solvent. And the surfaces of vesicles were rough and broken with THF as common solvent. The self-assembled nanostructures would be easily broken to release the cargos spontaneously, when they are used for drug release system. Therefore, we chose DMSO as the prominent common solvent to investigate the host-guest chemistry with β-cyclodextrins and redox-responsive release of model molecules in following sections.

Self-assembly of amphiphilic block copolymer with host molecule β-CD

Cyclodextrins (CDs) are a series of natural cyclic oligo-saccharides composed of D-glucose units that are connected by α-1,4-glucosidic linkages which can form inclusion complexes with a wide variety of guest species such as adamantane, ferrocene and *trans*-azobenzene in aqueous media.[90-91] The host-guest inclusion interactions are mainly governed by van der Waals forces and hydrophobic interactions, while the exterior hydroxyls of CDs improve their water solubility and bioavailability of the drugs. During the past few years, CDs and their derivatives have been recognized and frequently investigated as enzyme models and building blocks for the construction of supramolecular polymers in supramolecular chemistry. Furthermore, it's well known that β-CD can form stable 1:1 stoichiometric inclusion compounds with ferrocene and its derivatives in the reduced state, while exhibits a low affinity with ferrocene in its oxidized state. [92-93] Kaifer *et al.* have prepared a series of ferrocene-containing redox-active dendrimers, and further studied the interplay between host-guest molecular recognition and redox chemistry *via* multisite inclusion complexation with cyclodextrin.[94-98] Due to the hydrophilic nature of cyclodextrins' shell, cyclodextrins can be used to adjust the amphiphilicity of the polymer and phase separation process of self-assembly system. Yuan *et al* developed a host-controlled dynamic supramacromolecular self-assembly approach to build reversible ethyl cellulose-g-poly-(caprolactone)-*b*-poly(ethylene oxide) (EC-*g*-PCL-*b*-PEG) polymer architectures with α-CD from micelles to cylinders to vesicles to sheets for "living" assemblies.[99]

Herein, we chose PEG_{45}-*b*-$PMAEFc_{38}$ diblock copolymer to study the effect of host molecules β-CD on the self-assembled morphologies. Different amounts of β-CD ([ferrocene groups]: [β-CD] = 1:0, 1:0.5, 1:1.0, and 1:3.0) were respectively added into DMSO solution of the ferrocene-containing block copolymer under stirring to complex with the ferrocene moieties in its hydrophobic cavity. The host-guest interactions between β-CD and ferrocene groups were investigated by UV-Vis spectra (**Fig. 6a**). PEG_{45}-*b*-$PMAEFc_{38}$ displays a typical absorption of ferrocenyl group at 450 nm in DMSO. Upon adding host molecules β-CD with a molar ratio of 0.5 : 1 (compared to the ferrocene moieties), the absorption peak at 450 nm is

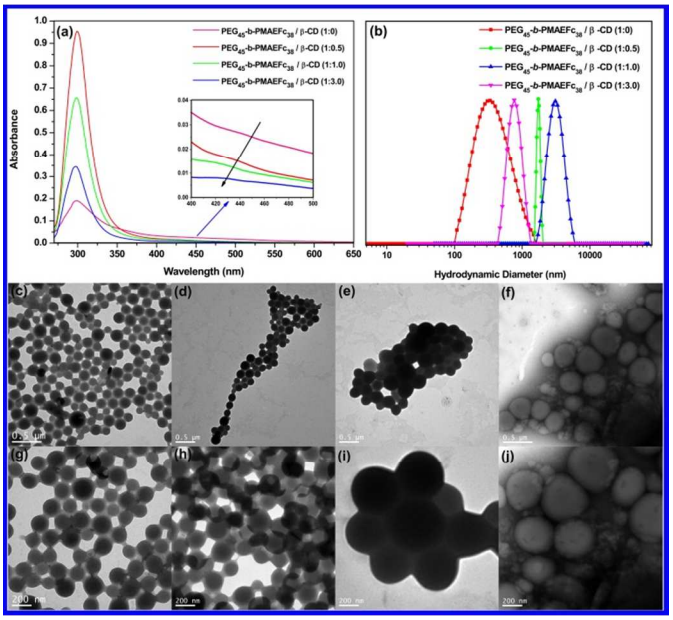

Fig. 6. UV-Vis spectra (a), DLS results (b) and TEM images of micelles formed by PEG_{45}-*b*-$PMAEFc_{38}$ with 0 (c, g), 0.5 (d, h), 1.0 equiv (e, i) , and 3.0 equiv (f, j) of β-CD based on ferrocene groups. (The scale bar of c-f is 0.5 μm; g-j is 200 nm)

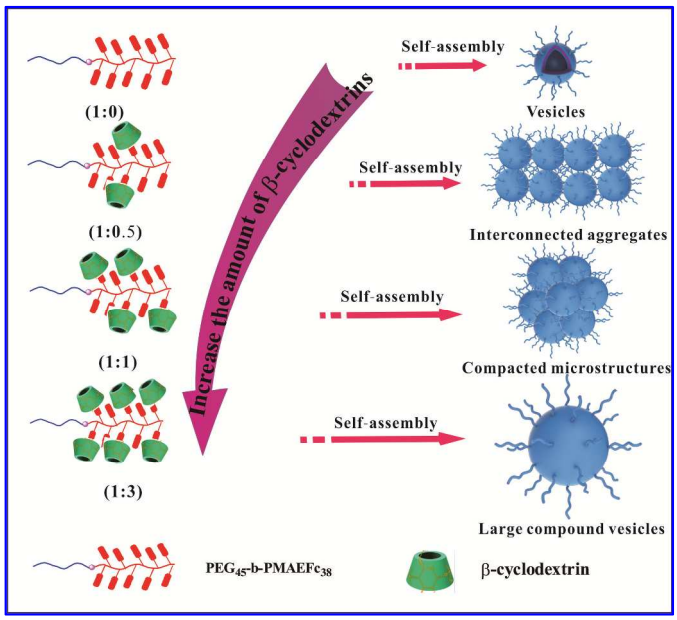

Scheme 3. The schematic illustration of the self-assembly process of PEG_{45}-*b*-$PMAEFc_{38}$ with addition of β-CD.

noticeably becomes less intense, clearly suggesting the formation of Fc/β-CD inclusion complexes. The absorption peak at 450 nm decreased with further increasing the molar ratio of β-CD to ferrocene moieties. In addition, the absorption peak assignable to ferrocene moieties in PEG_{45}-*b*-$PMAEFc_{38}$ are blue-shifted upon the addition of β-CD, perhaps due to the electron shift of ferrocene moieties induced by the high electron density in the cavity of β-CD. Thus, the change of the peaks is evidence for the host-guest interactions between β-CD and ferrocene moieties.[74-75] Changes in the morphology of amphiphilic block copolymer aggregates before and after the addition of different amounts of β-CD were visualized by TEM images. Without host-guest interactions with β-CD, PEG_{45}-*b*-$PMAEFc_{38}$ diblock copolymer can self-assemble into spherical vesicles of 350 nm in diameter as determined by DLS and TEM images as shown in **Fig. 6b**, **6c** and **6g**. With incorporation of host molecules β-CD with a molar ratio of 0.5 : 1 (compared to the ferrocene moieties) into diblock copolymer, the vesicles would interconnect together to obtain aggregates as revealed in the TEM images (**Fig. 6d** and **6h**). Upon further increasing the molar ratio of β-CD to ferrocene groups to 1:1, more compacted compound microstructures formed by spheres were facilely obtained as shown in **Fig. 6e** and **6i**. When the molar ratio of β-CD to ferrocene groups increased to 1:3, the compacted vesicles would undergo a fusion procedure, resulting in formation of single disperse vesicles. From the TEM images, we can find that the morphology changed from small vesicles to spheres to large vesicles, and the size of the single micelles formed *via* the self-assembly of PEG_{45}-*b*-$PMAEFc_{38}$ and β-CD complexes increased with increasing the content of β-CD. The addition of β-CD would increase the ratio of hydrophilic segments to hydrophobic segments, which can lead to the increase of repulsion in the corona and stretching in the core of single micelles of PEG_{45}-*b*-$PMAEFc_{38}$ copolymers. Interestingly, the single micelles would interconnect, compact and fuse with the addition of β-CD in the supramolecular systems due to intermolecular hydrogen bond interactions between the hydroxyls in β-CD. The DLS results of the supramolecular block copolymer aggregates are well agreeable with TEM results as shown in **Fig. 6b**. And the schematic illustration of the self-assembly process of PEG_{45}-*b*-$PMAEFc_{38}$ with addition of β-CD is shown in **Scheme 3.**

Redox-responsive self-assembly of PEG_{45}-*b*-$PMAEFc_{38}$ vesicles

The reversibly redox-responsive self-assembly of the block copolymer was also investigated *via* redox reactions of self-assembled vesicles using different chemical oxidants and reducing agents in water. Transmission electron microscopy (TEM) was used to visualize the redox-responsive self-assembly of the block copolymer. The obtained amphiphilic block copolymer PEG_{45}-*b*-$PMAEFc_{38}$ can self-assemble into vesicles in aqueous solution (**Fig. 7a**), which is stable for at least one month without any external stimuli. H_2O_2 and $KMnO_4$ were separately chosen as water-soluble oxidants to investigate the redox-responsive behavior of ferrocene segments in the aggregates and the consequent disassembly of the PEG_{45}-*b*-$PMAEFc_{38}$ vesicles. Upon oxidation with H_2O_2, the vesicles were broken to form the large aggregates (**Fig. 7b**) with a size of 618 nm. **Fig. 8** showed the UV-vis spectra of block copolymer in DMSO before and after oxidizing with excess H_2O_2. The absorption peak around 450 nm corresponding to ferrocene groups (in reduced form) almost disappeared after oxidizing with excess H_2O_2. With the increase of oxidants and time, the average hydrodynamic diameter of the aggregates increased obviously. The TEM results showed that aggregates grew up with a much larger size (**Fig. 7c**). We assume that the PMAEFc domains can be converted to poly(vinylferrocenium) domains upon oxidation, which are hydrophilic and therefore swollen in water. Additionally, the structure of the aggregates and the swelling of the poly(vinylferrocenium) domains after oxidation also depend on the kinds of oxidants we used. While treating with $KMnO_4$, the self-assembled vesicles would be selectively oxidized, and they shrank to from mesoporous-like vesicles with the diameter of 90 nm (**Fig. S8b** and **S8c**). As reported by Crespy *et al.*,[65] H_2O_2 diffuses faster than MnO_4^- in

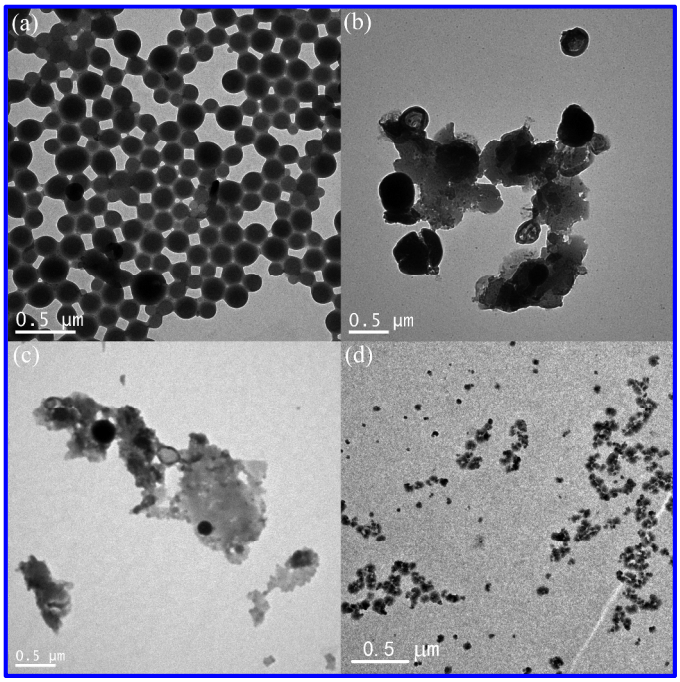

Fig. 7. The morphology of assembled PEG_{45}-*b*-$PMAEFc_{38}$ nanoparticles before oxidation (a); after oxidation with H_2O_2 equal amount of Fc units (b); excess of Fc units (c); reduction with ascorbic acid (d).

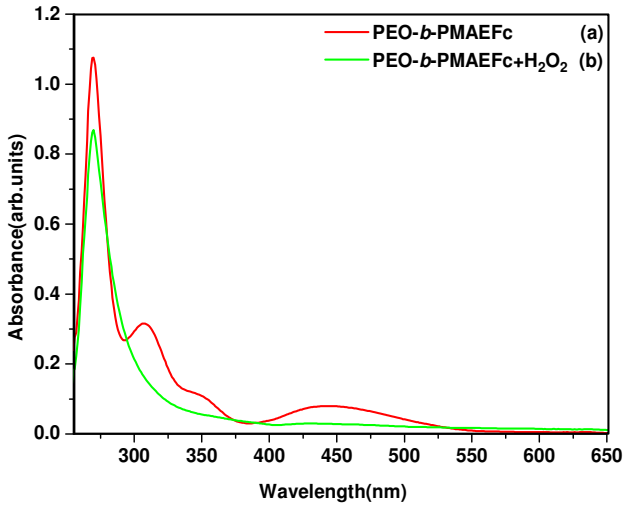

Fig. 8. The UV-Vis spectra of PEG_{45}-*b*-$PMAEFc_{38}$ block copolymer in DMSO (a) before and (b) after oxidation with excess H_2O_2.

the bilayer of the vesicles due to the ionic character of the latter, thus allowing a spatial rearrangement of the poly(vinyl ferrocenium) domains and a slight increase of the whole diameter of the aggregates. Second, the MnO_4^- may interact with the poly(vinylferrocenium) domains after the initial oxidation has taken place. MnO_4^- preferably oxidized ferrocene units spatially very close to poly(vinylferrocenium) side groups, and thus enhanced the local charge density. In contrast, H_2O_2 as a unipolar molecule may oxidize the PMAEFc side groups more effectively, which indicates the redox-responsive disassembly of block copolymer by H_2O_2 could be used to trigger the drug release system, since the concentration of H_2O_2 in the tumor is higher than that in normal tissues. [100-101]

In order to investigate the reversibility of redox-responsive self-assembly, the aggregates were reduced by the addition of ascorbic acid after being oxidized by H_2O_2 and $KMnO_4$. However, no significant changes in the diameter or in the morphology of the aggregates could be detected after the reduction with ascorbic acid, as shown by TEM micrographs (**Fig. 7d** and **Fig. S8d**). This indicated that the oxidation of the poly(vinylferrocene) block was possible, but the reduction was partially hindered due to the oxidized ferrocene moieties confined in the dense un-oxidized ferrocene domains. Overall, the oxidative-responsive behavior of the block copolymer micelles based on poly(vinylferrocene) provides an approach for stimuli-responsive and controlled drug delivery.

Encapsulation and redox release of fluorescence molecules

In order to investigate the redox-responsive ability of the ferrocene-containing block copolymer system, the assemblies of PEG_{45}-*b*-$PMAEFc_{38}$ were employed to encapsulate and sequentially release small fluorescence molecules upon an external oxidation stimulus. Rhodamine B (RB) was chosen as a simple model molecule and an imitative drug loaded in polymer vesicles to determine the release kinetics due to its unique fluorescence and hydrophilic characters. To assess the redox-responsive release behavior of the RB molecules upon addition of the oxidants, the RB-loaded PEG_{45}-*b*-$PMAEFc_{38}$ vesicles were prepared to perform controlled release experiments. The vesicular solution with H_2O_2 was dialyzed against a solution of H_2O_2 with same concentration. Thus, the release of RB was monitored by the increasing fluorescence of the solution outside the dialysis bag. A certain portion of deionized water solution was withdrawn from the beaker at certain time intervals. The solution was then placed into a cuvette to conduct fluorescence spectrum. The release rate of RB was calculated based on the fluorescence intensity. As shown in **Fig. 9**, a significant increase in fluorescence intensity with oxidation time of the vesicles with H_2O_2 was observed, indicating that RB was released from the micelles. We also found that the release of RB molecules from the sample without the treatment of oxidants. This is perhaps because RB can be absorbed

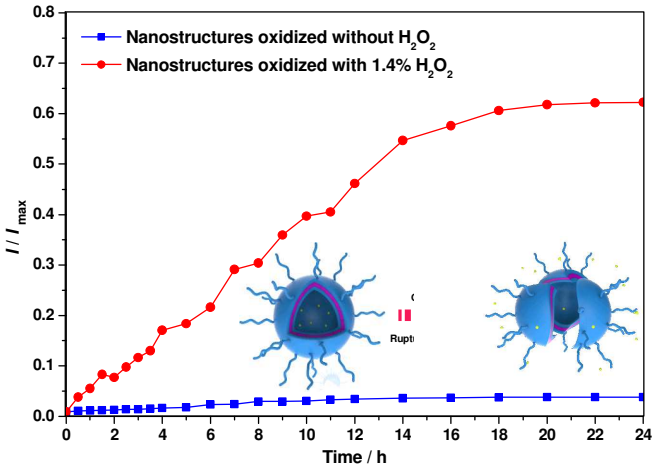

Fig. 9. Release kinetics of RB from PEG_{45}-*b*-$PMAEFc_{38}$ vesicles. The fluorescence intensity of the oxidized micelle increases with time, indicating a redox release of RB.

on the surface of the vesicles or slower released from the vesicles. Considering the important role of redox reactions in physiological environments, PEG-*b*-PMAEFc vesicles can be used in drug delivery systems to load functional molecules which can be released in a controllable manner upon oxidation stimuli.

Conclusions

In summary, redox-responsive ferrocene-containing amphiphilic block copolymers were synthesized using PEG-based macroATRP agent *via* ATRP, and can further self-assemble into a variety of nanostructures in aqueous solution. We have systematically studied the solution self-assembly behavior of PEG-*b*-PMAEFc amphiphilies, and found that the self-assembled morphologies are greatly dependent on the nature of the common solvent, polymer composition and concentration, and the addition of host molecule β-cyclodextrin (β-CD) and oxidants. Thus, we can achieve mutliple assembled morphologies including typical vesicles, flowerlike vesicles, large compound micelles (LCMs), interconnect-vesicles and mesoporous-like vesicles by changing the above factors. Moreover, the nanostructures fabricated from PEG-*b*-PMAEFc amphiphilies can disassemble upon external redox stimuli, especially for H_2O_2. Finally, the redox-responsive polymeric system was utilized for controlled release of a hydrophilic payload (RB) upon oxidation with H_2O_2, which plays an important role in specific physiological environment of tumor than normal tissues. We visualize that this redox-responsive ferrocene-containing block polymer system with particular morphologies would have potential applications in many fields, especially in stimuli-responsive drug delivery systems.

Acknowledgements

This work was financially supported by the National Natural Science Foundation of China (No. 21074035 and 51173044), Research Innovation Program of SMEC (No.14ZZ065), Shanghai Pujiang Program under 14PJ1402600 and the Project-sponsored by SRF for ROCS, SEM. W. Z. also acknowledges the support from the Fundamental Research Funds for the Central Universities.

Notes and references

Shanghai Key Laboratory of Advanced Polymeric Materials, East China University of Science and Technology, 130 Meilong Road, Shanghai 200237, P. R. China.

**Correspondence to: Weian Zhang (E-mail: wazhang@ecust.edu.cn)*

† Electronic Supplementary Information (ESI) available: Experimental details and characterization data. See DOI: 10.1039/c000000x/

1. D. E. Discher and A. Eisenberg, *Science*, 2002, 297, 967-973.
2. R. Savić, L. Luo, A. Eisenberg and D. Maysinger, *Science*, 2003, 300, 615-618.
3. M. A. C. Stuart, W. T. S. Huck, J. Genzer, M. Muller, C. Ober, M. Stamm, G. B. Sukhorukov, I. Szleifer, V. V. Tsukruk, M. Urban, F. Winnik, S. Zauscher, I. Luzinov and S. Minko, *Nat Mater*, 2010, 9, 101-113.
4. Y. Zhou, W. Huang, J. Liu, X. Zhu and D. Yan, *Advanced Materials*, 2010, 22, 4567-4590.
5. F. H. Schacher, P. A. Rupar and I. Manners, *Angewandte Chemie International Edition*, 2012, 51, 7898-7921.
6. S. Mura, J. Nicolas and P. Couvreur, *Nat Mater*, 2013, 12, 991-1003.
7. Z. Ge and S. Liu, *Chemical Society Reviews*, 2013, 42, 7289-7325.
8. J. Ding, X. Zhuang, C. Xiao, Y. Cheng, L. Zhao, C. He, Z. Tang and X. Chen, *Journal of Materials Chemistry*, 2011, 21, 11383-11391.
9. P. Schattling, F. D. Jochum and P. Theato, *Polymer Chemistry*, 2014, 5, 25-36.
10. C. M. Schilli, M. Zhang, E. Rizzardo, S. H. Thang, Y. K. Chong, K. Edwards, G. Karlsson and A. H. E. Müller, *Macromolecules*, 2004, 37, 7861-7866.
11. E. R. Gillies and J. M. J. Fréchet, *Bioconjugate Chemistry*, 2005, 16, 361-368.
12. J. Du and S. P. Armes, *Journal of the American Chemical Society*, 2005, 127, 12800-12801.
13. W. Xu, I. Choi, F. A. Plamper, C. V. Synatschke, A. H. E. Müller and V. V. Tsukruk, *ACS Nano*, 2012, 7, 598-613.
14. Y. Zhao, *Macromolecules*, 2012, 45, 3647-3657.
15. P. Han, S. Li, W. Cao, Y. Li, Z. Sun, Z. Wang and H. Xu, *Journal of Materials Chemistry B*, 2013, 1, 740-743.
16. Q. Xing, N. Li, D. Chen, W. Sha, Y. Jiao, X. Qi, Q. Xu and J. Lu, *Journal of Materials Chemistry B*, 2014, 2, 1182-1189.
17. H. Yamaguchi, Y. Kobayashi, R. Kobayashi, Y. Takashima, A. Hashidzume and A. Harada, *Nat Commun*, 2012, 3, 603.
18. S. Dai, P. Ravi and K. C. Tam, *Soft Matter*, 2009, 5, 2513-2533.
19. P. Zheng, X. Jiang, X. Zhang, W. Zhang and L. Shi, *Langmuir*, 2006, 22, 9393-9396.
20. Y.-Y. Li, X.-Z. Zhang, H. Cheng, G.-C. Kim, S.-X. Cheng and R.-X. Zhuo, *Biomacromolecules*, 2006, 7, 2956-2960.
21. J. Brassinne, J.-P. Bourgeois, C.-A. Fustin and J.-F. Gohy, *Soft Matter*, 2014, 10, 3086-3092.
22. D. Miyajima, F. Araoka, H. Takezoe, J. Kim, K. Kato, M. Takata and T. Aida, *Angewandte Chemie International Edition*, 2011, 50, 7865-7869.
23. Q. An, J. Brinkmann, J. Huskens, S. Krabbenborg, J. de Boer and P. Jonkheijm, *Angewandte Chemie International Edition*, 2012, 51, 12233-12237.
24. P. Zhang, L. Chen, T. Xu, H. Liu, X. Liu, J. Meng, G. Yang, L. Jiang and S. Wang, *Advanced Materials*, 2013, 25, 3566-3570.
25. Q. Yan, R. Zhou, C. Fu, H. Zhang, Y. Yin and J. Yuan, *Angewandte Chemie International Edition*, 2011, 50, 4923-4927.
26. Q. Yan and Y. Zhao, *Angewandte Chemie International Edition*, 2013, 52, 9948-9951.
27. S. S. Satav, S. Bhat and S. Thayumanavan, *Biomacromolecules*, 2010, 11, 1735-1740.
28. J. Zhang and B. Han, *Accounts of Chemical Research*, 2012, 46, 425-433.
29. Y. Zhao, K. Landfester and D. Crespy, *Soft Matter*, 2012, 8, 11687-11696.
30. L.-P. Lv, Y. Zhao, N. Vilbrandt, M. Gallei, A. Vimalanandan, M. Rohwerder, K. Landfester and D. Crespy, *Journal of the American Chemical Society*, 2013, 135, 14198-14205.

31. M. Nakahata, Y. Takashima, A. Hashidzume and A. Harada, *Angewandte Chemie International Edition*, 2013, 52, 5731-5735.
32. R. Dong, Y. Su, S. Yu, Y. Zhou, Y. Lu and X. Zhu, *Chemical Communications*, 2013, 49, 9845-9847.
33. M. Huo, J. Yuan, L. Tao and Y. Wei, *Polymer Chemistry*, 2014, 5, 1519-1528.
34. J. Kamada, K. Koynov, C. Corten, A. Juhari, J. A. Yoon, M. W. Urban, A. C. Balazs and K. Matyjaszewski, *Macromolecules*, 2010, 43, 4133-4139.
35. S. Samarajeewa, R. Shrestha, M. Elsabahy, A. Karwa, A. Li, R. P. Zentay, J. G. Kostelc, R. B. Dorshow and K. L. Wooley, *Molecular Pharmaceutics*, 2013, 10, 1092-1099.
36. M. Li, Z. Tang, H. Sun, J. Ding, W. Song and X. Chen, *Polymer Chemistry*, 2013, 4, 1199-1207.
37. C. Yuan, J. Guo, M. Tan, M. Guo, L. Qiu and F. Yan, *ACS Macro Letters*, 2014, 3, 271-275.
38. X. Ma and H. Tian, *Accounts of Chemical Research*, 2014.
39. Y. Ahn, Y. Jang, N. Selvapalam, G. Yun and K. Kim, *Angewandte Chemie International Edition*, 2013, 52, 3140-3144.
40. M. Nakahata, Y. Takashima and A. Harada, *Angewandte Chemie International Edition*, 2014, 53, 3617-3621.
41. A. Napoli, M. Valentini, N. Tirelli, M. Muller and J. A. Hubbell, *Nat Mater*, 2004, 3, 183-189.
42. T. Finkel and N. J. Holbrook, *Nature*, 2000, 408, 239-247.
43. J. Coyle and P. Puttfarcken, *Science*, 1993, 262, 689-695.
44. N. Ma, Y. Li, H. Xu, Z. Wang and X. Zhang, *Journal of the American Chemical Society*, 2009, 132, 442-443.
45. W. Cao, Y. Li, Y. Yi, S. Ji, L. Zeng, Z. Sun and H. Xu, *Chemical Science*, 2012, 3, 3403-3408.
46. H. Xu, W. Cao and X. Zhang, Accounts of Chemical Research, 2013, 46, 1647-1658.
47. W. Cao, Y. Gu, M. Meineck, T. Li and H. Xu, *Journal of the American Chemical Society*, 2014, 136, 5132-5137.
48. I. Manners, *Science*, 2001, 294, 1664-1666.
49. G. R. Whittell and I. Manners, *Advanced Materials*, 2007, 19, 3439-3468.
50. J.-C. Eloi, L. Chabanne, G. R. Whittell and I. Manners, *Materials Today*, 2008, 11, 28-36.
51. X. Wang, G. Guerin, H. Wang, Y. Wang, I. Manners and M. A. Winnik, *Science*, 2007, 317, 644-647.
52. H. Wang, W. Lin, K. P. Fritz, G. D. Scholes, M. A. Winnik and I. Manners, *Journal of the American Chemical Society*, 2007, 129, 12924-12925.
53. H. Qiu, G. Cambridge, M. A. Winnik and I. Manners, *Journal of the American Chemical Society*, 2013, 135, 12180-12183.
54. J. Qian, G. Guerin, Y. Lu, G. Cambridge, I. Manners and M. A. Winnik, *Angewandte Chemie International Edition*, 2011, 50, 1622-1625.
55. J. B. Gilroy, T. Gädt, G. R. Whittell, L. Chabanne, J. M. Mitchels, R. M. Richardson, M. A. Winnik and I. Manners, *Nat Chem*, 2010, 2, 566-570.
56. C. G. Hardy, L. Ren, T. C. Tamboue and C. Tang, *Journal of Polymer Science Part A: Polymer Chemistry*, 2011, 49, 1409-1420.
57. C. G. Hardy, L. X. Ren, T. Tamboue and C. B. Tang, *Abstracts of Papers of the American Chemical Society*, 2011, 241.
58. C. G. Hardy, L. Ren, J. Zhang and C. Tang, *Israel Journal of Chemistry*, 2012, 52, 230-245.
59. C. G. Hardy, L. Ren, S. Ma and C. Tang, *Chemical Communications*, 2013, 49, 4373-4375.
60. C. Feng, Z. Shen, D. Yang, Y. Li, J. Hu, G. Lu and X. Huang, *Journal of Polymer Science Part A: Polymer Chemistry*, 2009, 47, 4346-4357.
61. S. Zhai, J. Shang, D. Yang, S. Wang, J. Hu, G. Lu and X. Huang, *Journal of Polymer Science Part A: Polymer Chemistry*, 2012, 50, 811-820.
62. C. Feng, G. Lu, Y. Li and X. Huang, *Langmuir*, 2013, 29, 10922-10931.
63. M. Shi, A.-L. Li, H. Liang and J. Lu, *Macromolecules*, 2007, 40, 1891-1896.
64. Z.-P. Xiao, Z.-H. Cai, H. Liang and J. Lu, *Journal of Materials Chemistry*, 2010, 20, 8375-8381.
65. R. H. Staff, M. Gallei, M. Mazurowski, M. Rehahn, R. Berger, K. Landfester and D. Crespy, *ACS Nano*, 2012, 6, 9042-9049.
66. K. N. Power-Billard, R. J. Spontak and I. Manners, *Angewandte Chemie International Edition*, 2004, **43**, 1260-1264.
67. J.-C. Eloi, D. A. Rider, G. Cambridge, G. R. Whittell, M. A. Winnik and I. Manners, *Journal of the American Chemical Society*, 2011, **133**, 8903-8913.66.
68. G. Chen and M. Jiang, *Chemical Society Reviews*, 2011, 40, 2254-2266.
69. W. S. Jeon, K. Moon, S. H. Park, H. Chun, Y. H. Ko, J. Y. Lee, E. S. Lee, S. Samal, N. Selvapalam, M. V. Rekharsky, V. Sindelar, D. Sobransingh, Y. Inoue, A. E. Kaifer and K. Kim, *Journal of the American Chemical Society*, 2005, 127, 12984-12989.
70. Q. Duan, Y. Cao, Y. Li, X. Hu, T. Xiao, C. Lin, Y. Pan and L. Wang, *Journal of the American Chemical Society*, 2013, 135, 10542-10549.
71. J. Alvarez, Y. Wang, W. Ong and A. E. Kaifer, *Journal of Supramolecular Chemistry*, 2001, 1, 269-274.
72. Q. Shen, L. Liu and W. Zhang, *Langmuir*, 2014, 30, 9361-9369.
73. Q. Yan, J. Yuan, Z. Cai, Y. Xin, Y. Kang and Y. Yin, *Journal of the American Chemical Society*, 2010, 132, 9268-9270.
74. Q. Yan, A. Feng, H. Zhang, Y. Yin and J. Yuan, *Polymer Chemistry*, 2013, 4, 1216-1220.
75. L. Peng, A. Feng, H. Zhang, H. Wang, C. Jian, B. Liu, W. Gao and J. Yuan, *Polymer Chemistry*, 2014, 5, 1751-1759.
76. A. Feng, Q. Yan, H. Zhang, L. Peng and J. Yuan, *Chemical Communications*, 2014, 50, 4740-4742.
77. J. M. Harris and R. B. Chess, *Nat Rev Drug Discov*, 2003, 2, 214-221.
78. A. Kolate, D. Baradia, S. Patil, I. Vhora, G. Kore and A. Misra, *Journal of Controlled Release*, 2014, 192, 67-81.
79. G. R. Whittell, M. D. Hager, U. S. Schubert and I. Manners, *Nat Mater*, 2011, 10, 176-188.
80. M. Semsarilar and S. Perrier, *Nat Chem*, 2010, 2, 811-820.
81. K. Matyjaszewski, *Macromolecules*, 2012, 45, 4015-4039.
82. Y. Yang, Z. Xie and C. Wu, *Macromolecules*, 2002, 35, 3426-3432.
83. M. Gallei, *Macromolecular Chemistry and Physics*, 2014, 215, 699-704.
84. R. Dong, B. Zhu, Y. Zhou, D. Yan and X. Zhu, *Angewandte Chemie International Edition*, 2012, 51, 11633-11637.
85. Y. Mai and A. Eisenberg, *Chemical Society Reviews*, 2012, 41, 5969-5985.

86. L. Zhang and A. Eisenberg, *Journal of the American Chemical Society*, 1996, 118, 3168-3181.
87. L. Zhang and A. Eisenberg, *Science*, 1995, 268, 1728-1731.
88. X. Hu, J. Hu, J. Tian, Z. Ge, G. Zhang, K. Luo and S. Liu, *Journal of the American Chemical Society*, 2013, 135, 17617-17629.
89. H. Wang, A. J. Patil, K. Liu, S. Petrov, S. Mann, M. A. Winnik and I. Manners, *Advanced Materials*, 2009, 21, 1805-1808.
90. X. Liao, G. Chen and M. Jiang, *Polymer Chemistry*, 2013, **4**, 1733-1745.
91. M. E. Davis and M. E. Brewster, *Nat Rev Drug Discov*, 2004, 3, 1023-1035.
92. A. Harada and S. Takahashi, *Journal of the Chemical Society, Chemical Communications*, 1984, 645-646.
93. A. Harada and S. Takahashi, *Journal of Inclusion Phenomena*, 1984, 2, 791-798.
94. R. Isnin, C. Salam and A. E. Kaifer, *The Journal of Organic Chemistry*, 1991, 56, 35-41.
95. R. Castro, I. Cuadrado, B. Alonso, C. M. Casado, M. Morán and A. E. Kaifer, *Journal of the American Chemical Society*, 1997, 119, 5760-5761.
96. C. M. Cardona and A. E. Kaifer, *Journal of the American Chemical Society*, 1998, 120, 4023-4024.
97. A. E. Kaifer, *Accounts of Chemical Research*, 1998, 32, 62-71.
98. C. M. Cardona, S. Mendoza and A. E. Kaifer, *Chemical Society Reviews*, 2000, 29, 37-42.
99. Q. Yan, J. Yuan, Y. Kang and Y. Yin, *Polymer Chemistry*, 2010, 1, 423-425.
100. M. López-Lázaro, *Cancer Letters*, 2007, **252**, 1-8.
101. P. Prasad, C. R. Gordijo, A. Z. Abbasi, A. Maeda, A. Ip, A. M. Rauth, R. S. DaCosta and X. Y. Wu, *ACS Nano*, 2014, **8**, 3202-3212.

The synthesis and self-assembly of ferrocene-containing block copolymers PEG-*b*-PMAEFc, and the encapsulation and redox-responsive release of model molecule (rhodamine B) upon external redox stimuli (H_2O_2).